

UCRL-91503  
PREPRINT

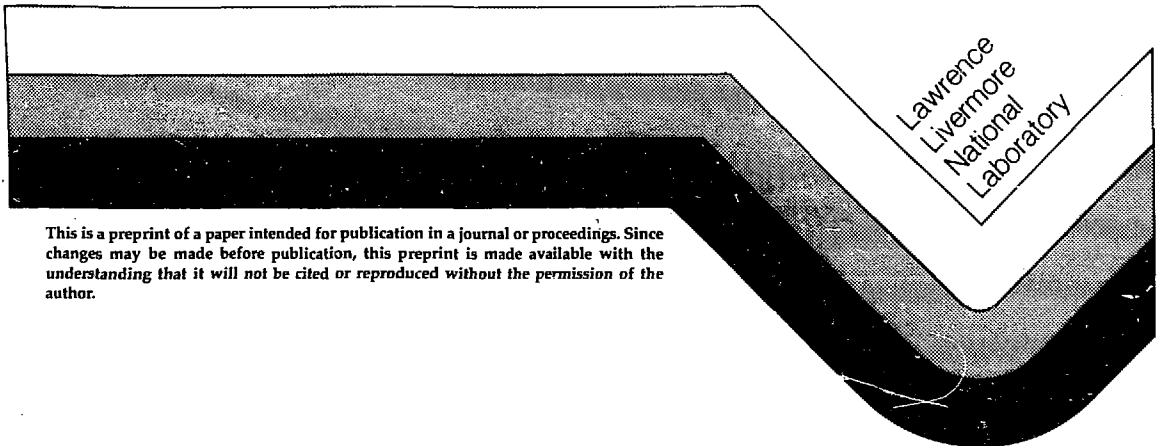
CONF-8409157--2

PERPENDICULAR ELECTRON CYCLOTRON EMISSION  
FROM HOT ELECTRONS IN TMX-II

R.A. James, R.F. Ellis, C.J. Lasnier,  
T.A. Casper, and C.M. Celata

This paper was prepared for submittal to the  
5th Topical Conference on High Temperature  
Plasma Diagnostics, APS, Lake Tahoe, CA,  
September 16-20, 1984.

September 14, 1984



This is a preprint of a paper intended for publication in a journal or proceedings. Since changes may be made before publication, this preprint is made available with the understanding that it will not be cited or reproduced without the permission of the author.

## PERPENDICULAR ELECTRON CYCLOTRON EMISSION FROM HOT ELECTRONS IN TMX-U

R.A. James, R.F. Ellis, C.J. Lasnier

University of Maryland, College Park, Maryland 20742

T.A. Casper

Lawrence Livermore National Laboratory, University of California

Livermore, CA 94550

C.M. Celata

Lawrence Berkeley Laboratory, University of California

Berkeley, CA 94720

## ABSTRACT

Perpendicular electron cyclotron emission (PECE) from the electron cyclotron resonant heating of hot electrons in TMX-U is measured at 30-40 and 50-75 GHz. This emission is optically thin and is measured at the midplane,  $f_{ce} \approx 14$  GHz, in either end cell. In the west end cell, the emission can be measured at different axial positions thus yielding the temporal history of the hot electron axial profile. These profiles are in excellent agreement with the axial diamagnetic signals. In addition, the PECE signal level correlates well with the diamagnetic signal over a wide range of hot electron densities. Preliminary results from theoretical modeling and comparisons with other diagnostics are also presented.

## INTRODUCTION

Electron cyclotron emission, also termed synchrotron radiation, results from electrons gyrating in a magnetic field.<sup>1</sup> In tokamaks, the low electron temperature ( $T_{eH} \lesssim 1$  keV) and known magnetic profile make it possible to determine the radial hot electron temperature profile.<sup>2</sup> In tandem mirrors with large plasma betas ( $\beta \geq 10\%$ ) and relativistic ( $T_{eH} \geq 100$  keV) anisotropic electron distributions, the emission spectrum is more complex. In this parameter range, modeling shows that electron cyclotron emission may be useful for determining the temporal evolution of the hot electron anisotropy, mean perpendicular energy and density.<sup>3</sup>

Perpendicular electron cyclotron emission (PECE) is currently measured at 35 GHz ( $\omega/\omega_{ce} \sim 2.5$ ) and 60 GHz ( $\omega/\omega_{ce} \sim 4.3$ ) in either end plug of TMX-U. In the west, polarization selection at 35 GHz is possible and the receiving horns can be aimed at different axial positions. Modeling has shown that 35 and 60 GHz emission is optically thin for TMX-U parameters.<sup>4</sup> In addition, recent analysis<sup>5</sup> shows that the diamagnetic loop signals (DML) in the end plugs are dominated by the hot electrons,  $DML \propto n_{eH} T_{eH}$ . This paper discusses some of the recently observed correlations between the diamagnetic signals and electron cyclotron emission from the hot electrons.

## SAMPLE SHOT

Figure 1 shows west end cell temporal signals from a shot used in the analysis of Figs. 3 and 4. The signals are (a) PECE at 35 and 60 GHz, (b) line density from an interferometer located 10 cm off the midplane, (c) input power from the fundamental ( $\omega_{ce}$ ) and second harmonic ( $2 \omega_{ce}$ ) ECRH gyrotrons, and (d) plasma diamagnetism located 38 cm and 94 cm off the

magnetic midplane. Note that both of the PECE signals and the diamagnetism (at 38 cm) do not decay like the interferometer signal. This suggests that the former are dominated by hot electrons,  $\tau_{\text{scatter}} > 500$  ms for  $T_{\text{eH}} > 100$  keV. The interferometer decay is the result of the rapid loss of cold plasma,  $T_e \lesssim 1$  keV, at the end of the shot.

#### CORRELATIONS WITH PLASMA DIAMAGNETISM

Differences in machine parameters such as ECRH power and timing, the gas fueling rate, and neutral beam power have produced parameter scans of the hot electrons' performance.

Figure 2 shows an excellent shot to shot correlation between the diamagnetism (at 38 cm) and the 35 and 60 GHz PECE signals at the end of the shot. X-ray data shows  $T_{\text{eH}} \simeq 250$  keV  $\pm$  50 keV, so the observed variation is mostly a change in the hot electron density,  $n_{\text{eH}}$ . The correlation shown in Fig. 2 implies that, like the DML signal, the PECE signal is dominated by the hot electrons.

#### AXIAL SCAN

By aiming the west plug receiving horn at different axial positions from shot to shot and averaging the results of several similar shots, an axial profile of the hot electrons is generated. This is shown in Fig. 3. Figure 1 is typical of the data used and the variation in the diamagnetism, interferometer, and ECRH power levels was less than 20% for all shots included in the analysis.

Since 35 GHz PECE is optically thin, the received signal is proportional to the path length through the plasma. This path length is determined by the plasma ellipticity and the angle at which the horn is aimed. The

signals in Fig. 3 have been corrected for the difference in path lengths relative to the emission at the midplane. The resulting signals are thus proportional to the hot electron density.

Note that the hot electron signal, proportional to density for optically thin emission, peaks at 14 cm off the midplane. This location is the on axis resonance ( $r = 0$ ) for second harmonic heating and is the position at which the second harmonic ECRH is aimed.

#### AXIAL PROFILE

To compare the data of Fig. 3 with the diamagnetic loop data, we will assume a gaussian axial profile for the hot electrons, centered about the magnetic midplane,  $n_{eH} = n_0 \exp[-(z/a_H)^2]$ , where  $a_H$  is the gaussian length or equivalently an e-folding length.

Noting that  $DML \propto n_{eH} T_{eH}/B^2$ , we calculated the temporal history of the gaussian length,  $a_H(t)_{DML}$ , by using the DML signals at 38 and 94 cm from the shot shown in Fig. 1. Analysis for  $t > 60$  ms was not performed because of noise problems in the 94 cm DML. Since the DML analysis assumes a peaked profile at the midplane, we ignore the PECE data at the midplane in Fig. 3, and use the remaining data to predict a second temporal history of the gaussian axial length,  $a_H(t)_{PECE}$ .

A comparison between these two profiles is shown in Fig. 4. Within the error bars ( $\pm 20\%$ ), the agreement is excellent, and shows that the axial profile is well represented by a gaussian for  $z \geq 14$  cm off the midplane. This is obviously not the case for  $z < 14$  cm. Thus, the PECE measurements can provide detailed information about the hot electrons near the midplane that cannot be observed by the diamagnetic loops.

#### ACKNOWLEDGMENT

Work performed for U.S. Department of Energy by University of Maryland under Contract AC05-77-ET53044, Lawrence Livermore National Laboratory under Contract W-7405-ENG-48, and Lawrence Berkeley Laboratory under Contract DE-AC03-76SF00098.

#### REFERENCES

1. G. Bekefi, Radiation Processes in Plasmas (John Wiley and Sons, Inc., New York, 1966).
2. M. Bornatici, R. Cano, O. DeBarbieri, and F. Engelmann, Nucl. Fusion 23, 1153 (1983).
3. D. Winske and D. A. Boyd, Phys. Fluids 26 (3) (1983).
4. C. M. Celata, Using Perpendicular Electron Cyclotron Emission to Diagnose the Thermal Barrier in TMX-Upgrade, submitted to Nuclear Fusion (1984).
5. E. Silver, Lawrence Livermore National Laboratory, Livermore, CA, private communication (1984).

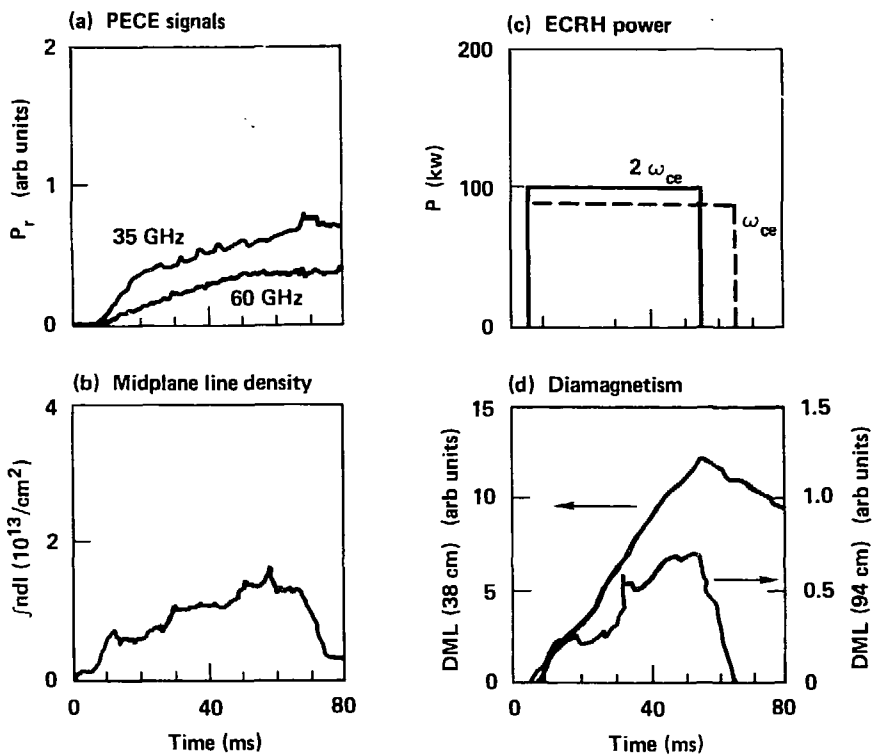
FIGURE CAPTIONS

Figure 1. Sample shot showing west plug temporal signals for (a) PECE at 35 and 60 GHz, (b) midplane interferometer line density, (c) ECRH gyrotron power, and (d) plasma diamagnetism.

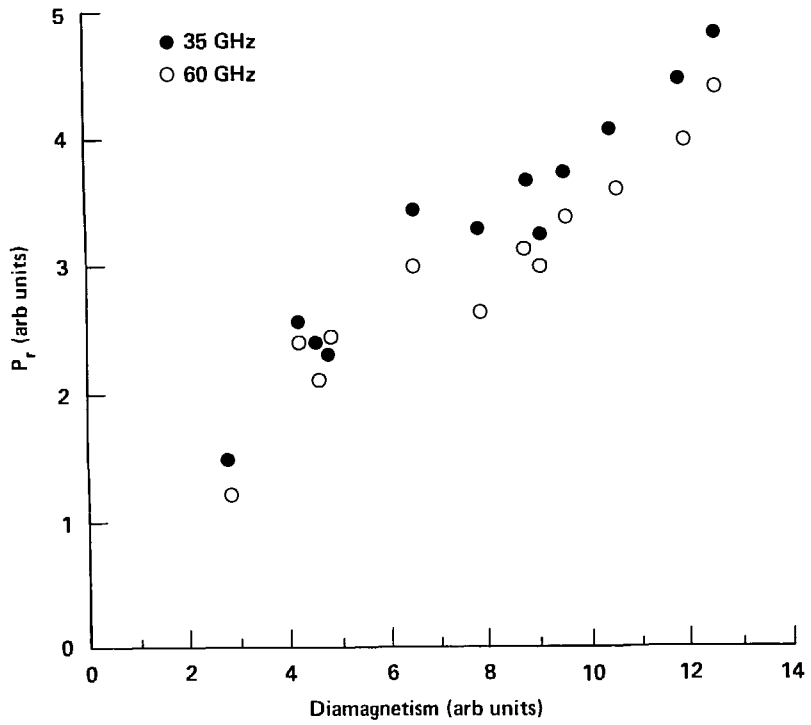
Figure 2. Shot to shot correlation between plasma diamagnetism and 35 and 60 GHz PECE signals.

Figure 3. Axial profile of 35 GHz signal.

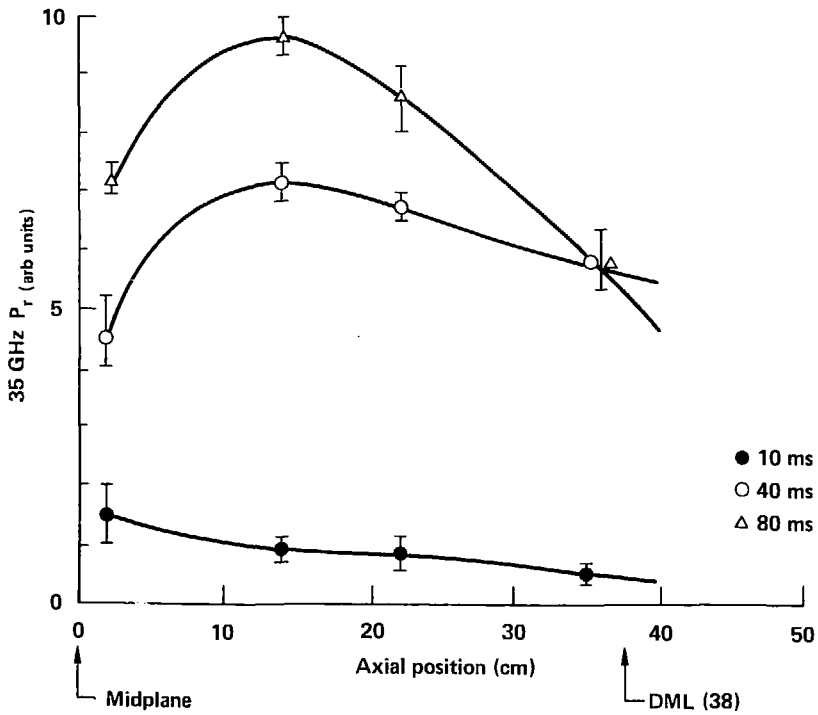
Figure 4. Predicted gaussian axial lengths from the diamagnetic loop signals and the PECE signals.



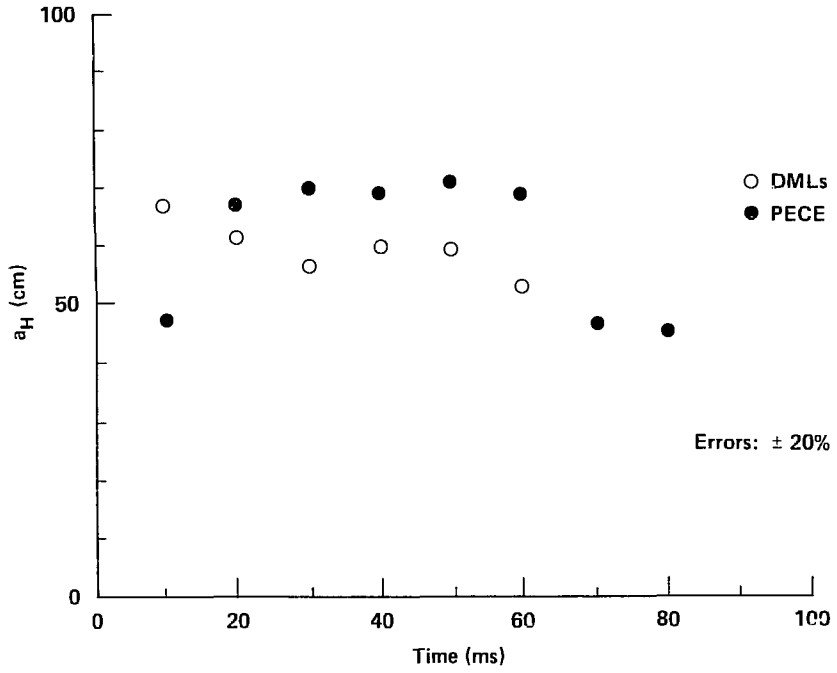
R. A. James et al. - Figure 2



R. A. James et al. - Figure 3



R. A. James et al. - Figure 4



## **DISCLAIMER**

This report was prepared as an account of work sponsored by an agency of the United States Government. Neither the United States Government nor any agency thereof, nor any of their employees, makes any warranty, express or implied, or assumes any legal liability or responsibility for the accuracy, completeness, or usefulness of any information, apparatus, product, or process disclosed, or represents that its use would not infringe privately owned rights. Reference herein to any specific commercial product, process, or service by trade name, trademark, manufacturer, or otherwise does not necessarily constitute or imply its endorsement, recommendation, or favoring by the United States Government or any agency thereof. The views and opinions of authors expressed herein do not necessarily state or reflect those of the United States Government or any agency thereof.